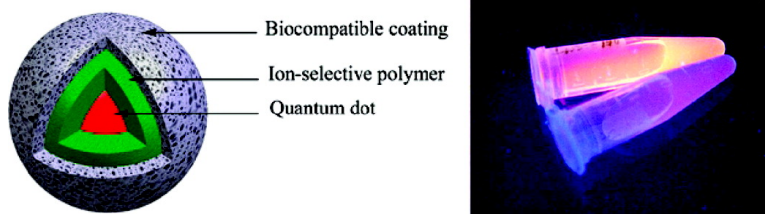


Ion-Selective Nano-optodes Incorporating Quantum Dots

J. Matthew Dubach, Daniel I. Harjes, and Heather A. Clark

J. Am. Chem. Soc., **2007**, 129 (27), 8418-8419 • DOI: 10.1021/ja072522l • Publication Date (Web): 14 June 2007

Downloaded from <http://pubs.acs.org> on February 16, 2009



More About This Article

Additional resources and features associated with this article are available within the HTML version:

- Supporting Information
- Links to the 1 articles that cite this article, as of the time of this article download
- Access to high resolution figures
- Links to articles and content related to this article
- Copyright permission to reproduce figures and/or text from this article

[View the Full Text HTML](#)



Ion-Selective Nano-optodes Incorporating Quantum Dots

J. Matthew Dubach, Daniel I. Harjes, and Heather A. Clark*

The Charles Stark Draper Laboratory, Bioengineering Group, 555 Technology Square, Cambridge, Massachusetts 02139

Received April 11, 2007; E-mail: hclark@draper.com

Quantum dots are attractive probes for microscopy because of their photophysical advantages,¹ particularly photostability and narrow bandwidth fluorescence emission with a wide excitation range. For *in vitro* and *in vivo* applications, they have found the greatest utility as inert markers^{2,3} and FRET-based sensors.^{2,4} Herein, we demonstrate a nanoscale ion-selective polymer-based sensor that incorporates quantum dots into the polymer matrix (ISQD). The composition imparts functionality to otherwise inert quantum dots, allowing the use of extremely bright probes for cellular ion measurements. The sensor is small, improving biocompatibility and response time, but still maintains a strong fluorescence signal from the quantum dots, which provide photostability and quantum efficiency. An idealized schematic of the sensor is shown in Figure 1a. The sensor comprises three-components: quantum dots, an ion-selective polymer matrix, and a biocompatible coating. The mechanism of the sensor is based on a combination of traditional ion-selective optodes and an innerfilter effect.

The ion-selective polymer that encases the quantum dots is based on traditional ion-selective optical sensors (optodes). The mechanism for optodes is well understood,⁵ and miniaturization to the nanoscale has been achieved.^{6,7} The polymer matrix contains a light absorbing pH indicator (chromoionophore) in conjunction with a nonabsorbing ion-binding molecule (ionophore). The chosen ionophore is selective for a particular ion, such as sodium, and extracts the ion from the solution into the polymer. As the positive charge is drawn into the matrix, a positive charge in the form of a hydrogen ion is released into solution, and the bulk pH of the sensing film is changed. Thus, the chromoionophore changes its color and the sodium concentration of the solution is measured indirectly. By exchanging the optode components, the selectivity and dynamic range can easily be modified. For instance, although we have illustrated a sodium-selective ISQD here, by exchanging the sodium-selective ionophore for one that is potassium selective, a potassium sensor can be produced.

The fluorescence of the embedded quantum dots is absorbed by the ion-selective polymer through a mechanism akin to a secondary innerfilter effect, such as that described in microdroplets.⁸ For molecular dyes, this has been well documented as a way to increase the signal intensity and concomitant sensitivity of ion-selective optical sensors.⁹ For ISQDs, the emission of the embedded quantum dots overlaps with the absorbance curve of the chromoionophore. As a result, the higher the absorbance is of the polymer, the greater the attenuation of fluorescence emission. The absorbance of the chromoionophore at 655 nm (gray lines, Figure 1b) decreases as sodium concentration increases, resulting in an increase in fluorescent signal directly related to increasing sodium concentration. Note the ideal overlap of the quantum dot emission (red line, Figure 1b), achieved because of the wide range of available choices and the narrow bandwidths of the quantum dots.

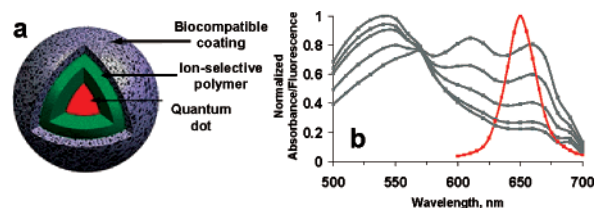


Figure 1. (a) Schematic of an ISQD, (b) spectral overlap.

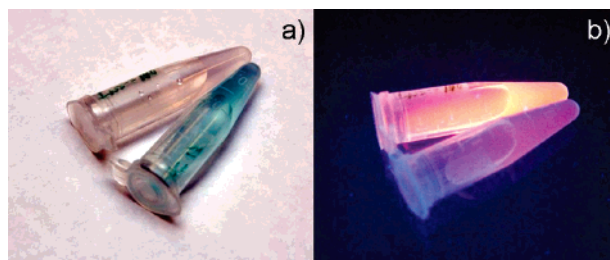


Figure 2. (a) Photograph of ISQDs in room light, (b) the same sample under UV excitation. ISQDs are contained in a 1.5 mL microcentrifuge tube.

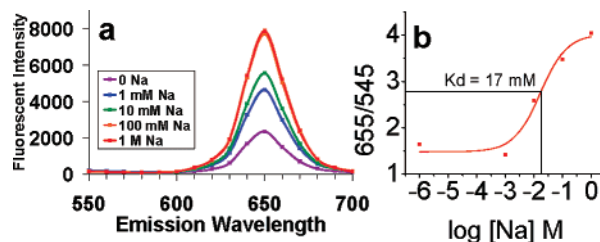


Figure 3. Experimental response to sodium: (a) spectral response of immobilized ISQDs to increasing concentrations of sodium; (b) calibration curve of ratiometric ISQDs.

Nanometer-sized ISQDs in solution, at the endpoints of the dynamic range, are shown in Figure 2. The absorbance changes from red to blue-green are easily seen by eye in Figure 2a. The same samples of nanosensors, but under UV excitation, are shown in Figure 2b. The polymer that was visually red does not absorb the 655 nm emission of the quantum dots and fluoresces brightly. The blue polymer absorbs the fluorescence emission of the quantum dot and has minimal emission.

To prevent dilution effects, the polymer matrix with no biocompatible coating was immobilized to a glass coverslip for calibration and selectivity measurements. The dynamic range of the sensor was found to be 1 mM to 1 M, shown spectrally in Figure 3a. By adjusting the ratio of components, the concentration range was tuned to maximize the resolution at typical levels of intracellular sodium. In this case, the resolution was 80 μ M at 17 mM, the center of the dynamic range. This means that a change in fluorescence intensity of 1% would correspond to a change in concentration of 80 μ M, as measured on a fluorescence plate reader. The center of the

dynamic range, 17 mM is a significant improvement over molecular indicators for sodium measurements, like Corona Green, with a Kd at 80 mM, which is higher than the intracellular range of sodium. As a control, no response to large changes in sodium concentration was observed when any one of the molecular components was removed. The incorporation of quantum dots improved the sensitivity of the nanosensors: those without quantum dots had a resolution of 370 μM .⁷

In addition, a ratiometric technique can be used by adding a second quantum dot color into the polymer matrix. An immobilized polymer matrix form of the ISQDs was formed containing quantum dots emitting at 545 and 655 nm, which are on opposite sides of the isosbestic point of the chromoionophore, Figure 1b. The results of this calibration, which are similar to that of the nonratiometric sensor, are shown in Figure 3b. Ratiometric measurements are useful for intracellular work, where it is difficult to control for dilution of sensors in the cytosol or concentration of sensors in organelles of the cell.

Also of note, even under several minutes of continuous excitation, minimal photobleaching was noted (data not shown). The absence of photobleaching in ISQDs allows, for example, fast kinetic measurements where experiments require continuous illumination. Currently, our focus is on short-term studies of cells in culture on the order of hours, and the ISQDs have been formulated accordingly. The leaching of components, specifically the ionic additive, from the polymer matrix affects the measurement after about a day in solution, and further studies would need to be done to reformulate the sensors for longer term experiments.

The selectivity of the sensor over potassium was determined by the separate solution method, Figure S1. In brief, the sensor was calibrated by the stepwise addition of sodium and compared to a parallel sensor calibrated by the stepwise addition of potassium. The distance between the two curves at $\alpha = 0.5$ is the selectivity of the analyte in the presence of the interfering ion. For the measurement of intracellular sodium, 10 mM, in the presence of intracellular potassium, 140 mM, a selectivity of at least two decades in concentration is required. Our sodium selective ISQDs display a selectivity of 2.3 decades, similar to that shown in micro-sized plasticized PVC particles using the same ionophore,¹⁰ meaning no interference from changes in potassium flux in our sodium measurements will be seen.

The sensors were prepared by sonicating a small amount of polymer cocktail in an aqueous solution of lipid-modified polyethylene glycol (PEG). The polymer matrix, owing to the extent of plasticizer it contains, is very lipophilic in nature. The lipid tail of the PEG molecule interacts with the sensor, leaving a monolayer of PEG on the surface of the nanosensor. The percent coverage was optimized by studying the ζ -potential of the nanoparticle suspension. Lipid-PEG molecules were added until the solution reached a maximum ζ -potential, at -27.5 mV. An ideal solution should have a ζ -potential close to -30 mV for maximum stability and thus minimization of particle aggregation. The final particle diameter, including the biocompatible coating, was determined to be 103 ± 2 nm. The small error associated with the average size demonstrates the batch reproducibility of ISQD formation. The particle size distribution, expressed by the standard deviation of an assumed Gaussian distribution, was determined to be 38 ± 2 nm. There are multiple quantum dots in each nanosensor, rather than the idealized example of one quantum dot at the core of a

polymer bead, as shown in Figure 1a. Not only is this a simple technique for covering the sensor with a biocompatible molecule, but it is easily modified to incorporate other PEG-lipid molecules. For instance, functionalized PEG lipids are commercially available, to which distinct chemistries could be added before sensor preparation. This has the potential to aid biocompatibility, cell loading, or intracellular targeting.

Early indications of cell biocompatibility have been noted from LIVE/DEAD assays which show no difference in viability from controls. Additionally, even over the course of 2 days, no obvious signs of apoptosis or necrosis have been observed. As further verification, the cytotoxicity was determined by incubating the nanosensors overnight with HEK 293 cells and measuring the degree of cellular injury with an MTT assay, Figure S2. The sodium ISQDs show no statistically significant cellular toxicity compared to controls over the course of 72 h after loading the ISQDs. The results also compared favorably to a similar concentration of gold nanoparticles, a particle that is generally accepted as biocompatible.

In summary, we have developed a bright, selective nanosensor that can measure physiologically relevant concentrations of sodium. This has the potential to be extended to other ions, such as potassium, calcium, chloride, etc. The sensors can easily be tuned to respond in different concentration ranges, depending on the intended application. Thus, it would be possible to measure ion flux in either the intracellular or extracellular environment by tuning the components accordingly. With a generalized biocompatible surface coating, the chemistry of the surface could be modified to enhance biocompatibility, enable cell loading, or stabilize the suspension.

Supporting Information Available: Experimental procedures, selectivity and biocompatibility data. This material is available free of charge via the Internet at <http://pubs.acs.org>.

References

- Bruchez, M., Jr.; Moronne, M.; Gin, P.; Weiss, S.; Alivisatos, A. P. *Science* **1998**, *281*, 2013–6. Chan, W. C.; Nie, S. *Science* **1998**, *281*, 2016–8.
- Alivisatos, A. P.; Gu, W.; Larabell, C. *Annu. Rev. Biomed. Eng.* **2005**, *7*, 55–76.
- Dubertret, B.; Skourides, P.; Norris, D. J.; Noireaux, V.; Brivanlou, A. H.; Libchaber, A. *Science* **2002**, *298*, 1759–62. Howarth, M.; Takao, K.; Hayashi, Y.; Ting, A. Y. *Proc. Natl. Acad. Sci. U.S.A.* **2005**, *102*, 7583–8. Jaiswal, J. K.; Mattoussi, H.; Mauro, J. M.; Simon, S. M. *Nat. Biotechnol.* **2003**, *21*, 47–51. Kim, S.; Lim, Y. T.; Soltesz, E. G.; De Grand, A. M.; Lee, J.; Nakayama, A.; Parker, J. A.; Mihajlovic, T.; Laurence, R. G.; Dor, D. M.; Cohn, L. H.; Bawendi, M. G.; Frangioni, J. V. *Nat. Biotechnol.* **2004**, *22*, 93–7. Michalet, X.; Pinaud, F. F.; Bentolila, L. A.; Tsay, J. M.; Doose, S.; Li, J. J.; Sundaresan, G.; Wu, A. M.; Gambhir, S. S.; Weiss, S. *Science* **2005**, *307*, 538–44.
- Medintz, I. L.; Clapp, A. R.; Mattoussi, H.; Goldman, E. R.; Fisher, B.; Mauro, J. M. *Nat. Mater.* **2003**, *2*, 630–8. Willard, D. M.; Carillo, L. L.; Jung, J.; Van Orden, A. *Nano Lett.* **2001**, *1*, 469–474.
- Seiler, K.; Simon, W. *Anal. Chim. Acta* **1992**, *266*, 73–87. Bakker, E.; Buhlmann, P.; Pretsch, E. *Chem. Rev.* **1997**, *97*, 3083–3132.
- Clark, H. A.; Hoyer, M.; Philbert, M. A.; Kopelman, R. *Anal. Chem.* **1999**, *71*, 4831–6. Clark, H. A.; Kopelman, R.; Tjalkens, R.; Philbert, M. A. *Anal. Chem.* **1999**, *71*, 4837–43. Brasuel, M.; Kopelman, R.; Miller, T. J.; Tjalkens, R.; Philbert, M. A. *Anal. Chem.* **2001**, *73*, 2221–8.
- Dubach, J. M.; Harjes, D. I.; Clark, H. A. *Nano Lett.* **2007**.
- Tohda, K.; Lu, H.; Umezawa, Y.; Gratzl, M. *Anal. Chem.* **2001**, *73*, 2070–2077.
- Gabor, G.; Walt, D. R. *Anal. Chem.* **1991**, *63*, 793–796. Shortreed, M.; Bakker, E.; Kopelman, R. *Anal. Chem.* **1996**, *68*, 2656–62. He, H.; Li, H.; Mohr, G.; Kovacs, B.; Werner, T.; Wolfbeis, O. S. *Anal. Chem.* **1993**, *65*, 123–127.
- Retter, R.; Peper, S.; Bell, M.; Tsagkatakis, I.; Bakker, E. *Anal. Chem.* **2002**, *74*, 5420–5.

JA072522L